

Mass Transfer Through Horizontal Liquid Films in Wavy Motion

SIMON L. GOREN and R. V. S. MANI

University of California, Berkeley, California

The effect of standing waves of controlled amplitude and frequency on the steady state rate of mass transfer through thin horizontal liquid layers is studied experimentally. The variables studied are the film thickness, the amplitude and frequency of the waves, and the spacing between the probes generating the waves. A bulk motion of complicated pattern known as drift is caused by the finite amplitude of the waves. The rate of mass transfer in the absence of imposed vibration is two to three times greater than that expected by molecular diffusion alone. Vibration increases the rate up to an order of magnitude or more, depending on the hydrodynamic conditions. The data at low frequencies are correlated by an expression of the form $(i-i_0)/i_{diff} = K\omega^{3/4}h^{1/2}L^{-1/2}$.

It is well known that liquid phase mass transfer rates in gas-liquid contacting may be significantly increased when waves appear on the interface. The increase is often very much more than can be accounted for by the increase in surface area alone. The increase in rate is to be sought, rather, in the interaction of the velocity and concentration fields, for if the instantaneous flux of a species in a fluctuating velocity and concentration field is given by $\bar{J} = -D\nabla\bar{c} + \bar{v}c$, then the averaged flux is given by $\bar{J} = -D\nabla\bar{c} + \bar{v}\bar{c} + \bar{v}'c'$. If the fluctuating velocity and fluctuating concentration have a component in phase the averaged flux will be increased by the convective terms even if the mean velocity is zero. Due to the smallness of the molecular diffusivity in liquids, the convective-eddy flux may be quite important in determining the overall transfer rate. A rigorous theory for the increase in mass transfer rate should be based on the convective diffusion equation using the velocity field set up by the waves, but due to the mathematical complexities of this problem and in computing the velocity field itself no adequate solution to the differential equation has been given yet. Instead, mass transfer across gas-liquid interfaces has been treated by idealized models such as surface renewals or eddy diffusion.

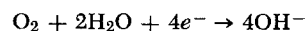
It would seem that experimental data on mass transfer rates in liquid films with waves of controlled amplitude and frequency would aid in the development of a more rigorous theory and in the evaluation of the various models. The only work known to the authors, however, where mass transfer was studied under the influence of waves of *controlled* frequency is that of Muenz and Marchello (8), who examined the unsteady state absorption of several gases into a horizontal layer of water on whose surface traveling waves of controlled frequency were generated. In their experiments reported so far, they made no attempt to vary the amplitude of the waves

or the depth of the liquid layer. They expressed their experimental results in terms of an effective diffusivity which they found to vary as the 7/6 power of the molecular diffusivity and the 1/3 power of the frequency. Two closely related problems are mass transfer into agitated pools (2, 5) and to falling liquid films (4, 6).

The present paper reports an experimental study of the effects of "standing waves" of *controlled* amplitude and frequency on the steady state mass transfer rate through thin horizontal liquid films. The system studied was oxygen transferring through aqueous potassium hydroxide solution and steady state was achieved by reducing the oxygen at limiting current at a horizontal cathode on the bottom of the liquid layer. The flux of oxygen was determined by measuring the current through the cathode. The variables studied were the film thickness, the frequency and amplitude of the waves, and the spacing between the probes generating the waves.

APPARATUS

Figure 1 gives a schematic representation of the apparatus. A silver electrode 60 to 70% by volume porous with cross section 14.5 cm. \times 7.5 cm. and thickness 0.127 cm. manufactured by the Clevite Corporation was supported in a Plexiglas trough whose inside horizontal cross section was slightly larger than that of the electrode. Silver was chosen as the cathode because this metal has been used extensively in the reduction of oxygen and the reaction is known to be



The trough was connected to another Plexiglas box which houses a nickel anode. It is necessary to separate the two electrodes, because the reverse reaction liberating oxygen takes place at the nickel anode and the liberated oxygen must be prevented from reaching the cathode. One normal aqueous potassium hydroxide was used as the electrolyte since extensive data on the solubility and diffusivity of oxygen in potassium

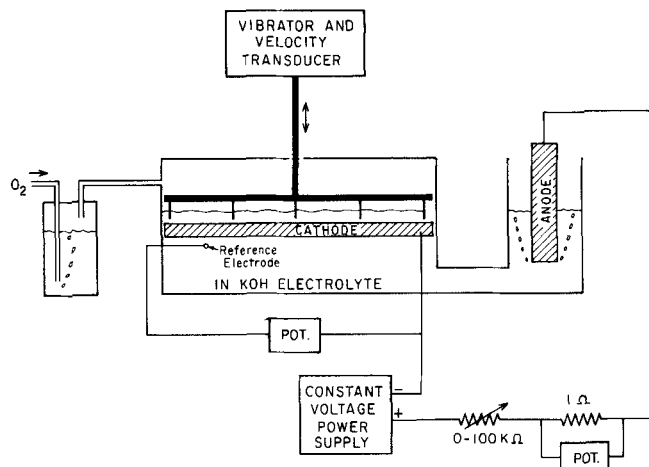


Fig. 1. Schematic of the apparatus.

hydroxide solutions are available (1). At 25°C. the solubility of oxygen in 1 N KOH in equilibrium with oxygen at 1 atm. pressure is 8.5×10^{-3} moles/liter and the diffusivity is 1.45×10^{-5} sq.cm/sec.

The cell was driven at constant current by a Heathkit Regulated Power Supply, Model IP-32 by taking a large potential drop across a 0 to 100 KΩ variable resistor. The resistance of the cell was found to be 1 KΩ. The current was controlled by varying the voltage output of the power supply (coarse scale) or by adjusting the variable resistor (fine scale). A silver-silver oxide reference electrode (3) was positioned on the underside of the cathode.

Waves were generated on the liquid surface by a probe that was driven by a Goodman vibrator (an electromagnet) and a sine wave generator. The shaft of the probe passed through a Sanborn velocity transducer, and since a feedback

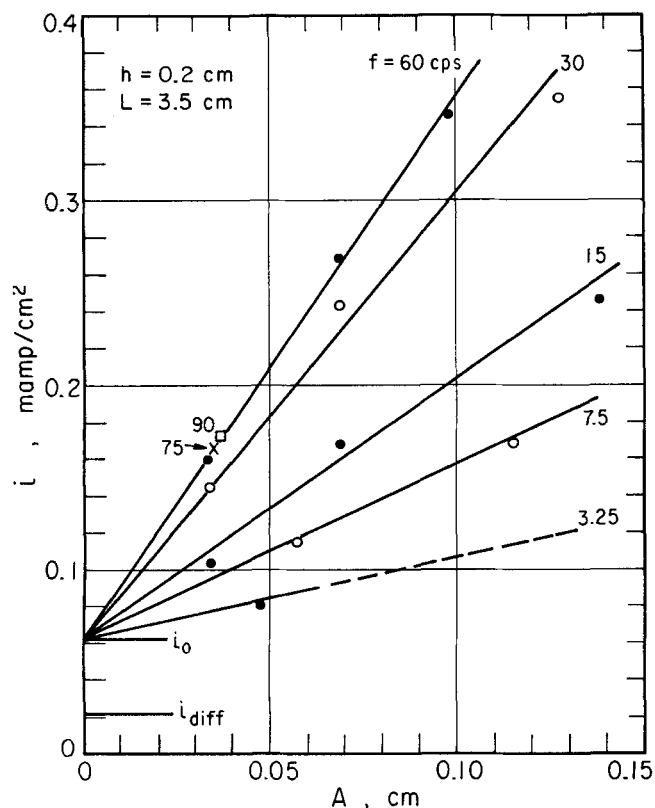


Fig. 2. Current density at limiting current as a function of probe amplitude. The film thickness is 0.2 cm. and the blade spacing is 3.5 cm.

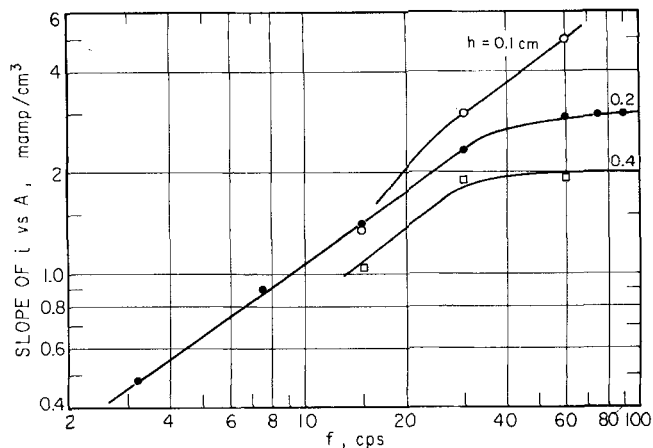


Fig. 3. Slopes of the lines i vs. A as a function of the frequency of vibration. The blade spacing is 3.5 cm.

circuit ensured that the velocity of the probe was sinusoidal, the amplitude of the probe displacement can be determined by dividing the amplitude of the velocity fluctuation as observed on an oscilloscope or chart recorder by the frequency of vibration and an empirical constant characteristic of the velocity transducer. The usable ranges of the probe were frequencies of 1 to 60 cycles/sec. and peak to peak amplitudes of 0 to 0.15 cm. The frequency of the waves was the same as that set on the sine wave generator. No attempt was made to measure the amplitude of the waves induced on the liquid surface. For purposes of data reduction the amplitude of the waves was taken to be proportional to the probe amplitude. In other experiments on vertical falling films with the same probe, it has been confirmed that the wave amplitude near the probe is proportional to the probe amplitude.

The probe itself was an inverted tee with five removable stainless steel blades 7.5 cm. \times 1 cm. \times 0.05 cm. attached at right angles to the horizontal base of the tee. With all five blades used, the spacing between blades was 3.5 cm. The housing supporting the probe and the trough were fitted with separate leveling screws to facilitate positioning and leveling the blades and the cathode. The thickness of the liquid layer above the cathode was determined with a cathetometer. The bottoms of the blades were positioned at about half the depth of the liquid film with a gap of about 0.1 cm. between the edges of the blades and the trough walls. The spacing between the blades and the walls was not varied, but might have an effect on the mass transfer rate if it changed the drift pattern. To eliminate gas phase resistance to the transfer, oxygen which was saturated with water by bubbling through 1 N KOH was passed over the top of the trough.

Steady state currents were determined for three film thicknesses, 0.1, 0.2, and 0.4 cm., both with and without vibration. Vibrations were imposed at frequencies of 15, 30, and 60 cycles/sec. and at three probe amplitudes, all with a blade spacing of 3.5 cm. In addition steady state currents were determined for the 0.2 cm. film at several other frequencies and at blade spacings of 7 and 15 cm. For each hydrodynamic condition the current density vs. cathode overpotential curves were traced near the limiting current region, allowing sufficient time for steady state to be achieved. Because of a slight slope in most of these curves, the limiting current is determined only to ± 0.05 mamp./sq.cm., that is, a maximum error of about 15%.

EXPERIMENTAL RESULTS

When the probe was vibrated two dimensional standing waves were observed on the liquid surface. These waves were parallel to the generating probes and there seemed to be little or no edge effect. Also, a mean motion was exhibited by small dust particles or dyed fluid. Such mean motion is to be expected as a result of the drift produced

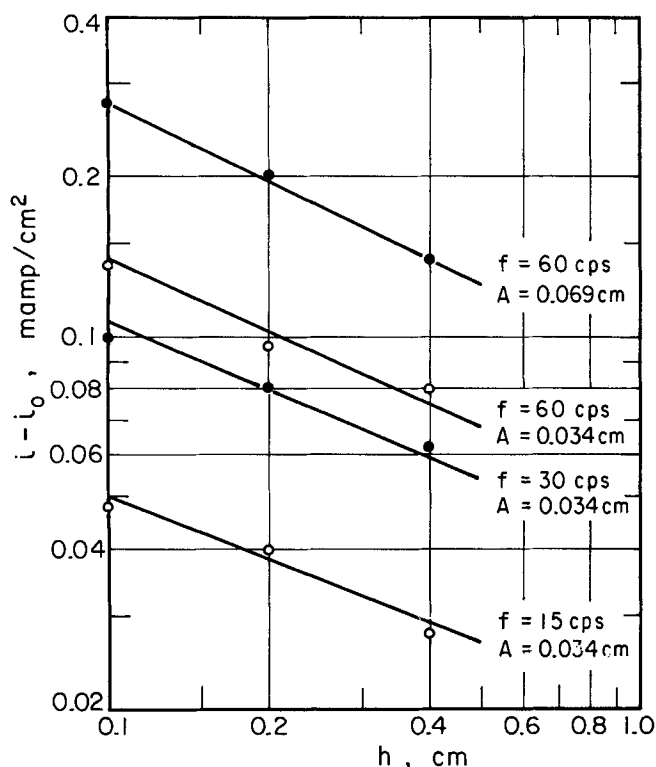


Fig. 4. Typical plots of the increase in current density as a function of film thickness. The blade spacing is 3.5 cm.

by the finite amplitude of the waves. The two-dimensional drift resulting from wave motion on thin horizontal liquid layers has been discussed most extensively by Longuet-Higgins (7). For the case of standing waves of wavelength λ , he showed that the mean motion will form cells of length $\frac{1}{4} \lambda$, adjacent cells rotating in opposite directions. There are velocity boundary layers of magnitude

$$\delta = (4\nu\omega/f)^{1/2} \quad (1)$$

at the top and bottom of the film. Just beyond the bound-

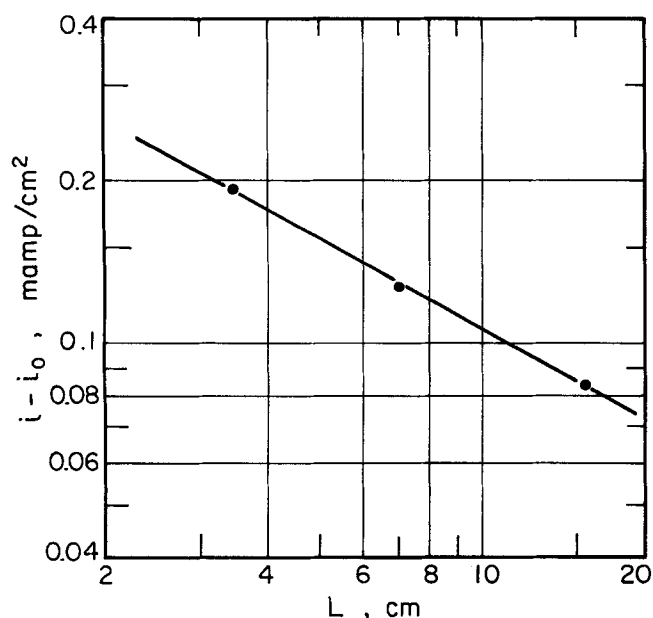


Fig. 5. Increase in current density as a function of blade spacing. The film thickness is 0.2 cm., the probe amplitude is 0.069 cm., and the frequency of vibration is 30 cycles/sec.

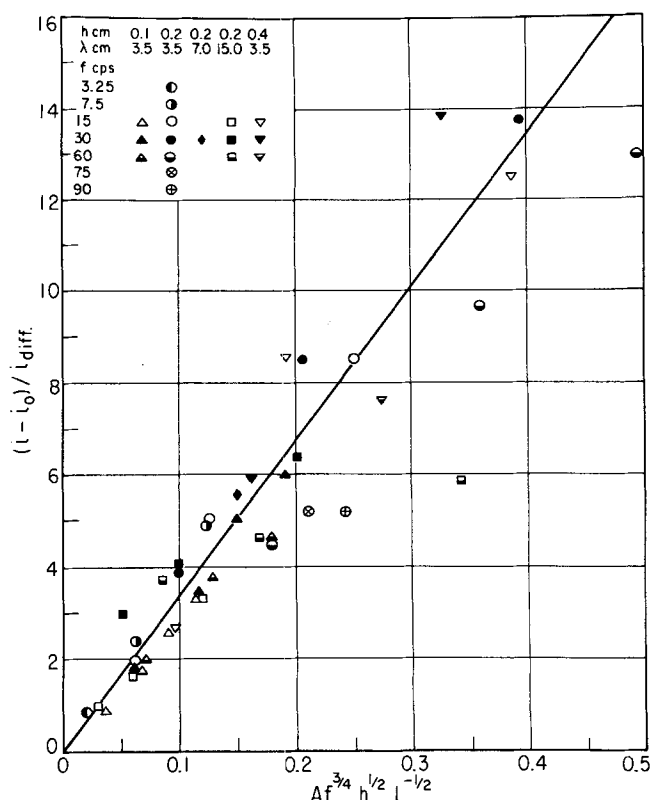


Fig. 6. Correlation for the increase in mass transfer rate for the lower frequency data.

ary layer on the bottom, Longuet-Higgins computes the velocity to be given by

$$\bar{U} = - \frac{3A^2f}{2\lambda \sinh^2(2\pi x/\lambda)} \sin(4\pi x/\lambda) \quad (2)$$

and just below the free surface the velocity gradient $\partial \bar{U} / \partial y$ vanishes. However, the observed motion did not agree with this two-dimensional representation. Instead, when viewed from above, vortices were observed in each right angle corner where a probe blade met the trough wall. The circulating flow around these vortices extended over the entire area between the two probes, but the velocity fell off as the distance from the corner increased. The velocity of circulation was observed to increase with increasing frequency and increasing amplitude in the range of variables studied, but this was not studied quantitatively. Apparently wall effects are very important in determining the geometrical pattern of the drift, but not in the wave pattern itself.

Figure 2 gives the observed current density at limiting current as a function of the imposed probe amplitude with the frequency of vibration as a parameter. The data in this figure are for the 0.2-cm. film and 3.5-cm. blade spacing and are typical of the data obtained under the other hydrodynamic conditions investigated. The current density expected due to molecular diffusion of oxygen alone is indicated on the ordinate. It was observed that even without vibration the current density was two to four times the expected value, and varied roughly as the $-\frac{1}{2}$ power of the film thickness instead of being inversely proportional to it as would be expected for molecular diffusion alone. In the experiments of Muenz and Marchello (8), the effective diffusivity of oxygen without pulsation was found to be 5.3 times larger than the molecular diffusion coefficient, whereas if our data are interpreted in terms of an effective diffusivity it would be two to four times larger than the molecular diffusion

coefficient depending on the film thickness. The somewhat greater effective diffusivity found by Muenz and Marchello may be due to their using deeper layers of liquid than in the present study which would be less effective in damping convection arising from room vibrations, density changes, or the Marangoni effect. Or it may be due to the fact that they performed unsteady state experiments where, because of the steeper concentration gradients, the effects of fluid motion on the mass transfer should be greater. Plevan (9) questions the manner in which Muenz and Marchello treat their data at long contact times to determine an effective diffusivity.

Whereas Muenz and Marchello explain their effective diffusivity in terms of surface driven convection, Plevan and Quinn (10) argue that the increase, for carbon dioxide at least, is buoyancy driven since experimental rates of desorption of carbon dioxide from water were in good agreement with theoretical calculations and with experimental rates of absorption into CMC gels, but were lower than rates of carbon dioxide adsorption into water. The density difference between the top and bottom of the liquid film necessary to initiate buoyancy-driven convection can be estimated from the critical Rayleigh number, $\Delta\rho gh^3/\rho\nu D$, which for a film with one solid interface and one free interface has the value 1.1×10^3 . For our thinnest film, $h = 0.1$ cm., we find the density difference must exceed 1.7×10^{-4} g./cc. for convection. It is not known whether the density difference between 1 N KOH saturated with oxygen and depleted of oxygen is of this order. Buoyancy-driven convection might also come about if there are significant variations in electrolyte concentration.

As indicated in Figure 2, almost all the data could be represented adequately by straight lines passing through the experimentally determined current density in the absence of vibration. This shows a first-power dependence of the increase in mass transfer rate with the imposed amplitude. Surprisingly, this simple relation holds even when the amplitude of the vibration approaches the film thickness! At low frequency the slopes of these lines increase with increasing frequency, but appear to approach a constant value at higher frequencies. This is shown in Figure 3 where the slopes of the lines i vs. A are plotted against the frequency of vibration for the three film thicknesses and for a blade spacing of 3.5 cm. The most extensive data were taken for the 0.2-cm. deep film for which the slopes vary as the $3/4$ power of the frequency up to 30 cycles/sec.

The increase in current density over that observed for no pulsation was plotted vs. the film thickness, all other parameters held constant. A typical diagram is shown in Figure 4. Most of the data when plotted this way indicated that the increase in mass transfer rate varied roughly as the $-1/2$ power of the film thickness.

The data taken for the 0.2-cm. film at a fixed frequency and fixed amplitude of vibration, but with varying blade spacing, gave a dependence of roughly the $-1/2$ power on the blade spacing for the increase in current density over that for no pulsation. This is shown in Figure 5.

Gathering these observations together and noting that the current density expected for molecular diffusion alone is

$$i_{\text{diff}} = 4FDc_s/h \quad (3)$$

we may write for the lower frequencies

$$(i - i_o)/i_{\text{diff}} = KAf^{3/4}h^{1/2}L^{-1/2} \quad (4)$$

The coefficient of proportionality should depend on the physical properties of the system, such as the molecular diffusion coefficient, the viscosity, the surface tension, . . . ,

and perhaps on the width of the trough which were not varied in the present study. In Figure 6 all the data obtained are plotted as $(i - i_o)/i_{\text{diff}}$ vs. $Af^{3/4}h^{1/2}L^{-1/2}$. Except for the data at frequencies above 60 cycles/sec. and the 60 cycles/sec. data for the 0.4-cm. deep film, the points fall on a fairly straight line. The figure shows that the vibration can increase the mass transfer rate over that expected by molecular diffusion alone by more than an order of magnitude. From the slope of this line the coefficient in Equation (4) is found to be $35 \text{ sec}^{3/4}/\text{cm}$. A more complicated correlation is needed to represent accurately the data at higher frequencies, and one possible form which reproduces the observed frequency dependence at both high and low frequencies is

$$(i - i_o)/i_{\text{diff}} = K_1Ah^{1/2}L^{-1/2}\{1 - \exp(-K_2f^{3/4})\}$$

Tentative values for K_1 and K_2 based on the present data are $K_1 = 4.3 \times 10^2 \text{ cm}^{-1}$ and $K_2 = 8.1 \times 10^{-2} \text{ sec}^{3/4}$.

DISCUSSION

The most surprising aspect of the present data is the first-power dependence of the increase in mass transfer rate with the imposed wave amplitude. For small amplitude waves both the increase in the area of the free surface and the drift velocity vary as the square of the amplitude. Moreover, we intuitively felt that the amplitude of the fluctuations in concentration should be roughly proportional to the velocity fluctuations, so that from the form of the averaged flux, $\bar{J} = -D\nabla\bar{c} + \bar{vc} + \bar{v'c'}$, we expected the increase in the steady state mass transfer rate to go as the square of the wave amplitude.

It was possible, however, to propose several highly speculative models which "predict" a first-power dependence of $(i - i_o)/i_{\text{diff}}$ on A . These models are based on a drift velocity of the form computed by Longuet-Higgins (7) for strictly two-dimensional motion:

$$\bar{U} = A^2f\lambda^{-1}F(2\pi h/\lambda, \dots) \quad (5)$$

Since the drift velocity was not measured in the present study and apparently is sensitive to the geometry of the probe and the wall, the exact form of Equation (5) is not known. In one model it is assumed that large-scale convective patterns with characteristic velocity \bar{U} and characteristic length L are set up and that the controlling zone for mass transfer is near the cathode; correlations for mass transfer from laminar flow to a flat plate are applied using \bar{U} and L as the characteristic dimensions, and since these correlations contain the $1/2$ power of the Reynolds number this introduces a first-power dependence of the increase in transfer rate on A . Similar results can be found using penetration theory with surface renewals with L/\bar{U} as the characteristic life time of the surface. In another model an attempt to take the fluctuating nature of the flow into account is made by introducing an eddy diffusivity near the cathode which is assumed to have the same form as that for turbulent flow, namely, $\epsilon(y) = \text{const } \nu y^{+3} = \text{const } u_\tau^3 y^3/\nu^2$; for $u_\tau = (\tau_w/\rho)^{1/2} = (\nu\partial\bar{U}/\partial y)^{1/2}$, we take $(\nu U/\delta)^{1/2}$ with δ given by Equation (1). None of the models was satisfying and they were not capable of predicting the observed dependence of $(i - i_o)/i_{\text{diff}}$ on the other variables.

We should mention that in some preliminary experiments with circular waves on thin films, a second-power dependence of $(i - i_o)/i_{\text{diff}}$ on A and a first-power dependence on f were suggested by the data. For this geometry the drift was observed to take place only in radial planes, and it may be that the detailed geometry of the probe and vessel wall are not important here in

determining the drift and the mass transfer.

For comparison with the present results, we reproduce the correlation suggested by Muenz and Marchello (8) giving the effective diffusivity \mathcal{D}_w for unsteady state mass transfer to a deep liquid layer with traveling waves on the free surface:

$$\mathcal{D}_w/\mathcal{D} = 2.74 (\nu/\mathcal{D})^{-1/6} (fh^2/\nu)^{1/3}$$

Owing to the differences in experimental conditions, namely, traveling waves vs. standing waves, deep liquid layers vs. thin films, and unsteady state transfer vs. steady state transfer, there is no obvious reason to expect the same dependence of the increase in mass transfer rate on the various parameters.

ACKNOWLEDGMENT

This work was supported by the National Science Foundation through Grant GP2763. The authors wish to acknowledge R. Zane of the Lawrence Radiation Laboratory (Berkeley) for the design of the probe drive and its associated electrical circuitry.

NOTATION

- A = peak-to-peak probe amplitude, cm.
 \mathcal{D} = molecular diffusivity, sq.cm./sec.
 f = wave frequency, sec.⁻¹
 h = thickness of liquid layer, cm.
 i = current density at limiting current, mamp./sq.cm.
 i_o = observed current density with no vibration,

mamp./sq.cm.

- i_{diff} = current density expected due to molecular diffusion only, mamp./sq.cm.
 K = empirical constant, sec.^{3/4}/cm.
 L = spacing between probe blades, cm.
 \bar{U} = drift velocity, cm./sec.
 δ = boundary-layer thickness, cm.
 λ = wavelength, cm.
 ν = kinematic viscosity, sq.cm./sec.

LITERATURE CITED

1. Davis, R. E., G. L. Horwath, and C. W. Tobias, *Electrochemical Acta*, to be published.
2. Dobbins, W. E., "International Conference on Water Pollution Research," Vol. 2, Paper No. 20-1, London (1962).
3. Ives, D. J. G., and G. J. Janz, "Reference Electrodes, Theory and Practice," Chap. 7, Academic Press, New York (1961).
4. Jepsen, J. C., O. K. Crosser, and R. H. Perry, *AIChE J.*, **12**, 186 (1966).
5. Kozinski, A. A., and C. J. King, *ibid.*, **12**, 109 (1966).
6. Levich, V. G., "Physicochemical Hydrodynamics," Chap. 12, Prentice Hall, Englewood Cliffs, N. J. (1962).
7. Longuet-Higgins, M. S., *Roy. Soc. London Phil. Trans.*, **245**, 535 (1953).
8. Muenz, Kurt, and J. M. Marchello, *AIChE J.*, **12**, 249 (1966).
9. Plevan, R. E., private communication.
10. Plevan, R. E., and J. A. Quinn, *AIChE J.*, **12**, 894 (1966).

Manuscript received December 13, 1966; revision received May 1, 1967; paper accepted May 2, 1967.

A Kinetic Approach for Polymer Solution Data

H. T. KIM and ROBERT S. BRODKEY

The Ohio State University, Columbus, Ohio

The phenomenological theory previously presented for describing the rheological properties of non-Newtonian materials was applied to two polymer solution systems. The basic shear diagram is needed over a wide range of shear rates and polymer concentrations, and such data are not readily available; however, what could be found supported the analysis. In order to confirm the theory further, ten solutions of polymethylmetacrylate in diethylphthalate with concentrations up to 55% were investigated at 40°C. The results indicated that the forward and reverse orders were 1 and 2 respectively and that the two parameters of the theory (a susceptibility to shear term and an equilibrium type of constant) were constant over the range of concentrations investigated. The flow data were reproduced to within a few percent for all solutions, although the errors were large for the very dilute concentration, where experimental difficulties precluded obtaining reliable data. The method allows correlation of polymer solution data over the range from lower to upper Newtonian viscosities and over a wide concentration range.

The rapid development of polymer science in the past twenty years has much to do with the present emphasis on the study of rheology. Most polymers known today behave as non-Newtonian fluids do, and a knowledge of their rheological behavior has become essential for good design such as in predicting the power input and the flow patterns in operations like mixing, extrusion, and molding. Many investigators have attempted to explain the basic reasons why these substances exhibit non-Newtonian flow

behaviors. On a macroscopic scale these explanations may involve phenomena such as agglomeration or other particle interactions as a function of shear and time. On a microscopic basis, they may involve such molecular interactions as entanglement, dipole attraction, hydrogen bonding, or other forms of association. Furthermore, average molecular weight, molecular weight distribution, and structure of the material such as branching and the type of radicals in the branching will also contribute to this behavior. These effects and possibly others result in the

H. T. Kim is with Goodrich Chemical Company, Avon Lake, Ohio.